Genet. Res., Camb. (2000), **76**, *pp.* 135–147. *With* 8 *figures.* Printed in the United Kingdom © 2000 Cambridge University Press

Unusual inheritance of the *Axin^{Fu}* mutation in mice is associated with widespread rearrangements in the proximal region of chromosome 17

ANATOLY RUVINSKY[1]*, WARREN D. FLOOD[1], TONG ZHANG[2] AND FRANK COSTANTINI[2]

[1] *Animal Science, SRSNR, University of New England, Armidale, NSW 2351, Australia*
[2] *Department of Genetics and Development, Columbia University, New York, NY 10032, USA*

(*Received 18 January 2000 and in revised form 6 March 2000*)

Summary

Axin^{Fu} is a mutation in mice that causes fused tails and other developmental abnormalities as a result of insertion of an intracisternal-A particle (IAP), a murine retrotransposon, into intron 6. In a small percentage of offspring we found that the mutant allele reverts to wild-type through loss of the insertion with concomitant disappearance of the mutant phenotype. Investigation of a series of microsatellite loci in the proximal region of chromosome 17 revealed novel alleles which arise simultaneously with disappearance of IAP from *Axin^{Fu}*. These novel microsatellite variants are distinct from the parental alleles and those so far discovered are organized into two haplotypes. Both haplotypes demonstrate stable Mendelian inheritance. Results show that these rearrangements, which are involved in the production of the new haplotypes, exceed millions of base pairs.

1. Introduction

Axin^{Fu} is a mutation in mice which causes kinked, fused tails and other developmental abnormalities including axial duplications (Reed, 1937; Dunn & Gluecksohn-Waelsch, 1954; Greenspan & O'Brien, 1986; Ruvinsky *et al.*, 1991). The *Axin* gene is located proximally on chromosome 17 and encodes a component of the Wnt signalling pathway (Hart *et al.*, 1998; Ikeda *et al.*, 1998; Kishida *et al.*, 1998), an important regulator of embryonic axis formation in mammals (Zeng *et al.*, 1997). The mutant *Axin^{Fu}* allele results from insertion of an intracisternal-A particle (IAP), a murine retrotransposon, into intron 6 of the *Axin* gene (Perry *et al.*, 1995; Vasicek *et al.*, 1997). This mutant allele is able to produce wild-type transcript, as well as mutant transcripts, arising from either alternative splicing or initiation of transcription from a cryptic promoter. It has been suggested that the mutant gene leads to the fused phenotype through a gain-of-function effect (Greenspan & O'Brien, 1986; Ruvinsky *et al.*, 1991; Perry *et al.*, 1995), possibly by encoding a hyperactive form of Axin protein (Hsu *et al.*, 1999).

Axin^{Fu} exhibits an unusual pattern of inheritance (Belyaev *et al.*, 1981). In previous experiments around 1–5% of offspring in test crosses which were expected to be *Axin^{Fu}* heterozygotes had a normal phenotype and did not transmit the mutation to the next generation (Ruvinsky, 1987). This is clearly distinct from low penetrance, which is typical for this mutation, as such mice are able to produce phenotypically mutant offspring in the next generation.

Gene conversion, being a basic genetic process, has been intensively investigated over the last few decades (Holliday, 1964; Szostak *et al.*, 1983; Pittman & Schimenti, 1998). More recently, data have appeared concerning mammalian genetic systems which demonstrate gene conversion (Bollag *et al.*, 1992; Giver & Grosovsky, 1997). It has become clear that gene conversion is able to cover significant regions of chromosome (< 1 cM) and may generate clustered mutations within the conversion tract. This extends the current understanding of the role of gene conversion, which was traditionally considered to be a

* Corresponding author. Tel: +61 (02) 67 73 3900. Fax: +61 (02) 67 73 3275. aruvinsk@metz.une.edu.au

major mechanism in the reduction of genetic variability. Gap-filling synthesis, being a component of gene conversion, has been shown to be error-prone in some cases and is a likely cause of new mutations (Giver & Grosovsky, 1997; Richard *et al*., 1999).

In this study we show that the unusual mode of *Axin*^{Fu} inheritance results from disappearance of the IAP insertion from the mutant allele. Surprisingly it was found that this process coincides with widespread reorganization of the proximal region of chromosome 17. Our data may indicate that gene conversion-like events account for disappearance of the IAP and the widespread reorganization of the proximal region of chromosome 17 in mice.

2. Materials and methods

(i) *Mice*

Strains 129/Rr *Axin*^{Fu}/+ and TF/Le (*tf*/*tf*) were obtained from the Jackson Laboratory (USA). The main breeding regime used in this study was *Axin*^{Fu}+/+*tf*×+*tf*/+*tf*. DNA was isolated from 0·5 cm tail cuttings by phenol/chloroform extraction following overnight digestion with proteinase K.

(ii) *PCR amplification*

Multiplex reactions consisted of primer P23 (5′cggagctattccgagaacg3′) which is specific for exon 6 of *Axin*, G245.R1 (5′gaccagagcccaagaaaaaccc3′) which targets intron 6 of *Axin* and IAP-F (5′gcgcatcactccctgattg3′) which anneals the long terminal repeats of the IAP insertion. An additional primer, RP2 (5′ctggttgttgtgttcttcc3′), was used in conjunction with P23 in standard PCR to characterize the 5′ region of IAP insertion. $MgCl_2$ concentration was 1·5 mM and reactions were performed on a MJ Research PTC-200 Peltier thermal cycler. Thermal parameters consisted of 30 cycles of 94 °C for 30 s, 58 °C for 10 s, and 72 °C for 80 s. PCR products were electrophoresed on 2% agarose gels and stained with ethidium bromide.

(iii) *Southern blot*

Genomic DNA was digested with *Pst*I and fractionated by agarose gel electrophoresis. Southern blot was hybridized with a ^{32}P-labelled, 240 bp *Pst*I–*Kpn*I fragment of *Axin* cDNA, which contained portions of exons 6 and 7. This probe hybridizes with a single 802 bp band from wild-type DNA and two bands of 508 and 660 bp from *Axin*^{Fu} DNA.

(iv) *Cloning and sequencing*

Amplified sequences were cloned into pBluescript II (Strategene) using the TA strategy (Marchuk *et al*., 1991) and constructs were transformed into $CaCl_2$-induced DH5α competent cells. Sequences were generated in both directions with primers T3 and T7 using an Applied Biosystems Catalyst 877 thermal cycler. Automatic sequencing was performed on an Applied Biosystems 377 sequencer. Samples were run for between 7 and 8 h through a 4% polyacrylamide gel.

(v) *Microsatellite markers*

Microsatellites *D17Mit19*, *D17Mit164*, *D17Mit113*, *D17Mit78*, *D17Mit133*, *D17Mit100*, *D17Mit173*, *D17Lon7*, *D17Mit80*, *D17Mit30 and D17Mit191* were investigated in this study. Primers for these microsatellites were obtained from Research Genetics (Huntsville, AL), except for *D17Lon7* (Fisher Biotec). One microlitre DNA samples (20–50 ng) were aliquoted into 0·2 ml microfuge tubes. Nine microlitres of pre-prepared reaction mix was subsequently added to the sample and overlaid with 15 μl mineral oil. $MgCl_2$ concentration was 3 mM. Thermal cycling was performed on a MJ Research PTC-200 Peltier thermal cycler incorporating a touchdown protocol. The parameters were 95 °C for 2 min followed by 30 cycles of 95 °C for 45 s, 60 °C for 45 s–0·5 °C/cycle, 72 °C for 1 min. A final incubation of 72 °C for 7 min was also performed. [^{32}P]αdATP was incorporated during amplification. Products were electrophoresed on a 5% polyacrylamide gel and exposed to Biomax MR film (Kodak).

3. Results

(i) *Disappearance of IAP*

The genetic map of the region under investigation on chromosome 17 indicates the location of the *Axin* and *tufted* loci (Fig. 1*A*). The recessive mutation *tufted* was used as a reliable genetic marker to trace transmission of the homologous chromosomes. In test crosses *Axin*^{Fu}+/+*tf*×+*tf*/+*tf*, one can expect that half of the progeny will carry *Axin*^{Fu} and the other half will be +*tf*/+*tf* homozygotes. As previously described, one can also expect that some offspring carrying *Axin*^{Fu} would have a normal tail phenotype due to decreased penetrance of the allele (Belyaev *et al*., 1981). These animals would not express the tufted trait because of their heterozygosity for the recessive *tf* allele. Rare cases of recombination between the *Axin* and *tufted* loci are also anticipated. Accordingly we employed polymorphic microsatellite markers to identify reciprocal recombination events that may have taken place in the region and thus distinguish recombination from other possible chromosomal rearrangements.

https://doi.org/10.1017/S0016672300004651 Published online by Cambridge University Press

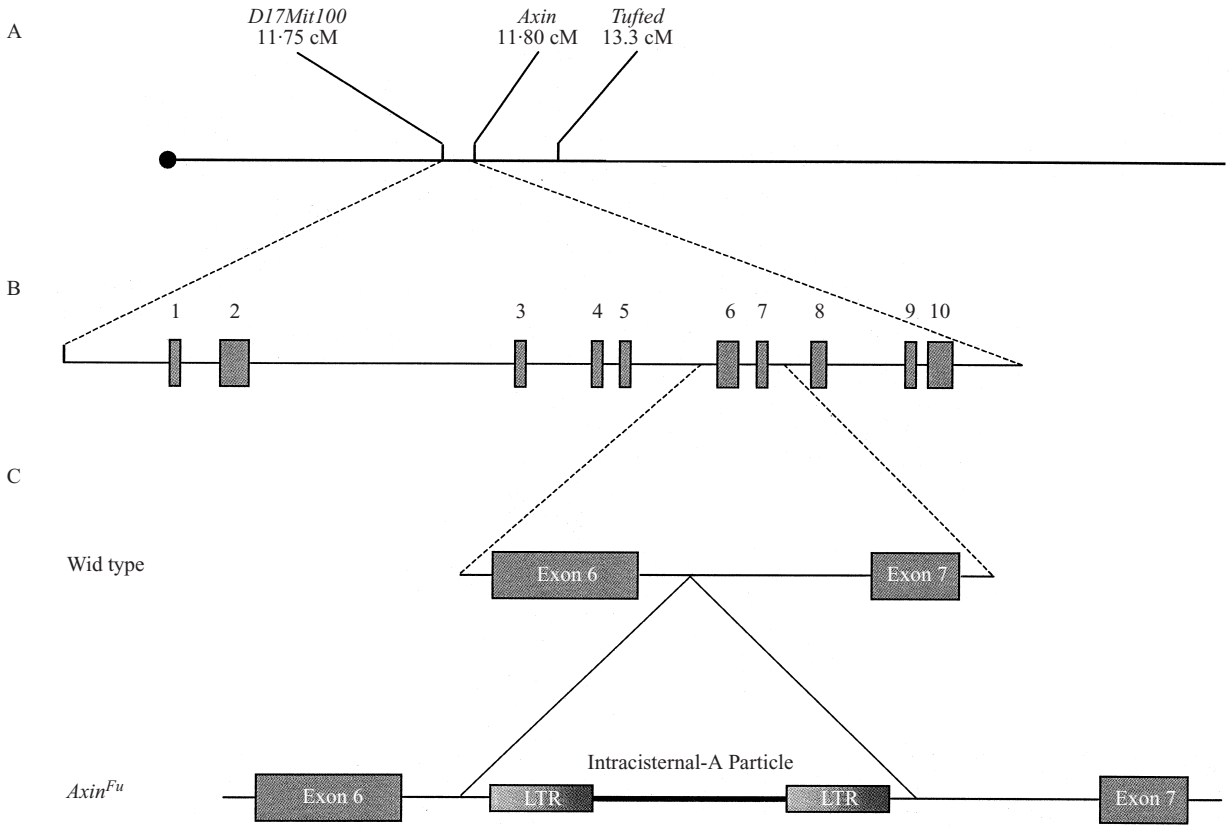

Fig. 1. (*A*) Genetic map (not to scale) of the proximal region of chromosome 17. Locus *D17Mit100* is located approximately 5 kb upstream from exon 1 of *Axin*. (*B*) Physical map (not to scale) of the *Axin* gene. Numbers indicate exons. (*C*) Structure of intron 6 in the wild-type and mutant *Axin*^{Fu} alleles. Intracisternal A-particle (IAP) is inserted into intron 6 of *Axin*^{Fu} in the opposite transcriptional orientation to *Axin*.

It was earlier shown that *Axin*^{Fu} + / + *tf* × + *tf* / + *tf* crosses produced small numbers of offspring that did not express *Axin*^{Fu} and did not pass this mutation to the following generation (Belyaev *et al*., 1981). Such mice were described as 'inactivants' and represented as [*Axin*^{Fu}]/ + (Belyaev *et al*., 1981). Using this cross we observed 22 non-fused, non-tufted offspring from a total of 1380 studied. These mice were descended from six different families and were derived from phenotypically fused parents who carried the *Axin*^{Fu} allele. These non-fused, non-tufted mice did not transmit the *Axin*^{Fu} allele to their offspring across at least two or three consecutive generations, clearly distinguishing them from mice with low penetrance. The genotypes of these two phenotypically similar groups of offspring were distinct, as determined by PCR.

The *Axin*^{Fu} allele differs from wild-type (Fig. 1 *B*, *C*) due to the IAP insertion into intron 6 (Vasicek *et al*., 1997; Zeng *et al*., 1997). PCR was used to investigate the presence of the IAP insertion in the non-fused, non-tufted mice. Primers P23 and G245.R1 amplify a region from the wild-type *Axin* allele covering a part of exon 6 and intron 6, while primers IAP.F and G245.R1 amplify a fragment from mutant allele *Axin*^{Fu} covering the 3′ end of the IAP and part of intron 6 (Fig. 2 *A*).

Multiplex reactions with primers P23, IAP-F and G245.R1 were employed to investigate mice with genotypes + / +, *Axin*^{Fu} / +, *Axin*^{Fu} / *Axin*^{Fu} (Fig. 2 *B*, lanes 1–3). Wild-type homozygotes generate a single fast-migrating band (252 bp) (designated F), while *Axin*^{Fu} homozygotes generate a single slow-migrating band (341 bp) (designated S), due to amplification between IAP.F and G245.R1. Accordingly heterozygotes generate both bands. All studied [*Axin*^{Fu}]/ + mice generated only a 252 bp, fast-migrating band (Fig. 2 *B*, lane 4) typical for wild-type. This provided an initial indication that the IAP is absent from chromosomes carrying the [*Axin*^{Fu}] allele. Southern blot analysis confirmed the loss of IAP from intron 6. *Axin*^{Fu} homozygotes and wild-type homozygotes displayed the expected bands for alleles with and without the IAP insertion, respectively, while heterozygotes displayed both (Fig. 2 *C*, lanes 1–3). The structure of the locus in [*Axin*^{Fu}]/ + individuals was identical to wild-type, showing only the wild-type band (Fig. 2 *C*, lane 4).

To determine the DNA structure around the IAP insertion in the *Axin* alleles studied, we cloned and sequenced the products of multiplex PCR. In addition we cloned and sequenced the amplification product between primers P23 and RP2 from the *Axin*^{Fu} allele

https://doi.org/10.1017/S0016672300004651 Published online by Cambridge University Press

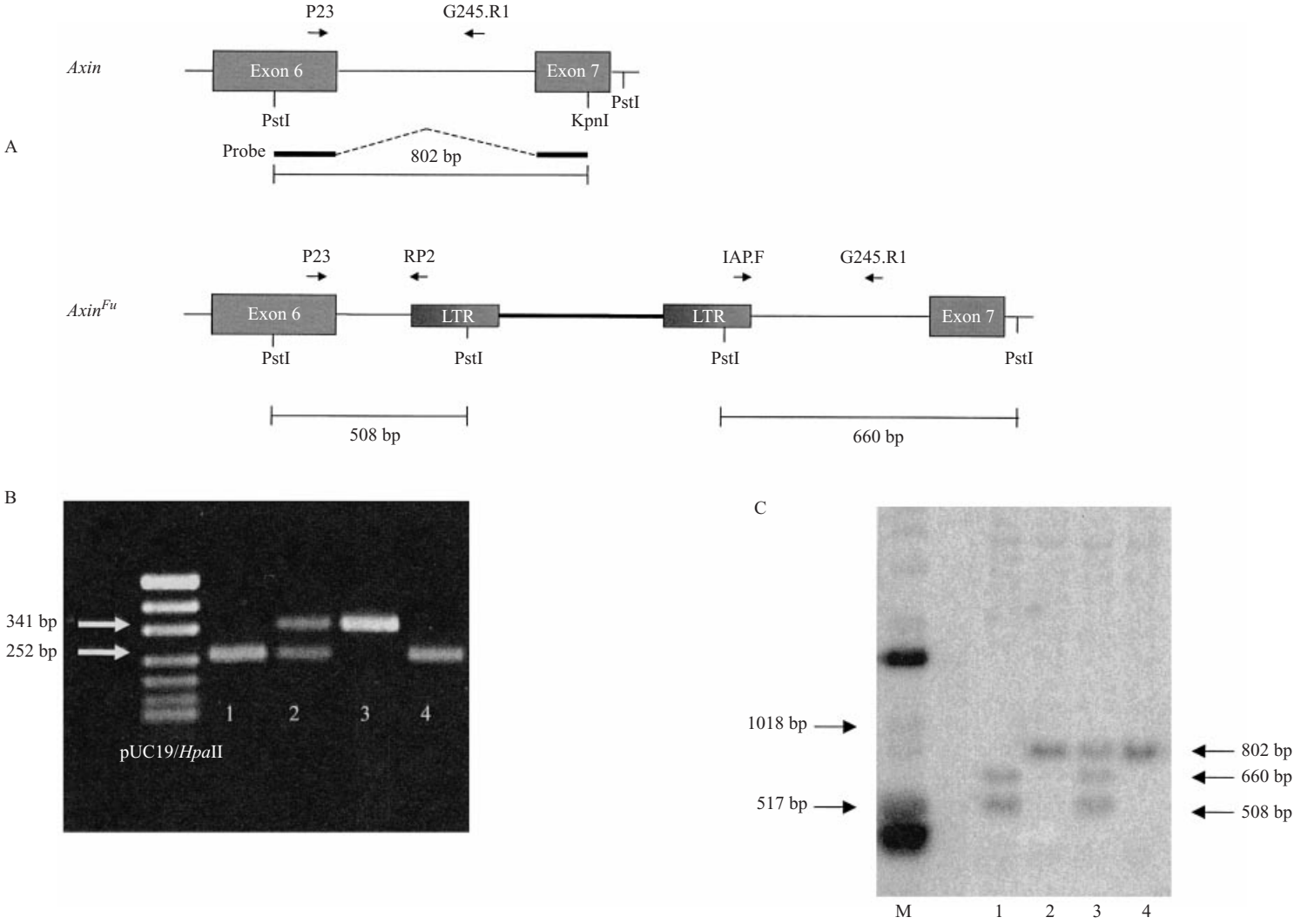

Fig. 2. (*A*) PCR and Southern blot schemes. Upper: PCR primers P23 and G245.R1 amplify a 252 bp product from the wild-type allele. Amplification between IAP.F and G245 in $Axin^{Fu}$ generates a longer 341 bp product. Lower: Schematic representation of the Southern blot strategy differentiating the structure of wild-type and $Axin^{Fu}$ alleles. The cDNA probe targets exons 6 and 7 in both wild-type and mutant alleles. Dashed line indicates spliced intron. (*B*) Two per cent agarose gel of *Axin* PCR products from different genotypes. Multiplex reactions were performed using primers P23, IAP-F and G245.R1. Lane 1, $+/+$; lane 2, $Axin^{Fu}/+$; lane 3, $Axin^{Fu}/Axin^{Fu}$; lane 4, $[Axin^{Fu}]/+$. (*C*) Southern blot of the different genotypes. The 508 and 660 bp bands indicate the IAP insertion in the $Axin^{Fu}$ allele while the 802 bp band denotes the wild-type allele. Lane M, molecular weight markers; lane 1, $Axin^{Fu}/Axin^{Fu}$; lane 2, $+/+$; lane 3, $Axin^{Fu}/+$; lane 4, $[Axin^{Fu}]/+$.

A

5′**CGGAGCTATTCCGAGAACG**CAGGCACCACCCTCAGTGCTGGGGATTTGGCC
TTTGGGTGAGTCTTGATCCAGCCTTCTTAATGTT***TCCAGT***GTGTCCTTGTAT
CCAAGTCATGGTTCATCGAGTCCGTGGTCCTGTGGTGACTTAATCCAGTCAA
AGTCAGACAATACCCGGGCCAGGGGCCAGTCAGACTCCAGGCCTTGCTATGA
CTGGATGAGGAGGGGCGCACTTTGGGTTTTTCTTGGGCTCTGGTC 3′

B

5′**CGGAGCTATTCCGAGAACG**CAGGCACCACCCTCAGTGCTGGGGATTTGGCC
TTTGGGTGAGTCTTGATCCAGCCTTCTTAATGTT***TCCAGT***tgttattagacg
cgttctcacgaccggccaggaagaacacaacaaccag 3′

C

5′gcgcatcactccctgattggctgcagcccatggccgagctgacgttcacgg
gaaaaacagagtacaagtggtcgtaaatacccttggctcatgcgcagattat
ttgtttaccaacttagaacacaggatgtcagcgccatcttgtgacggcgaat
gtgggggcggcttcccaca***TCCAGT***GTGTCCTTGTATCCAAGTCATGGTTCA
TCGAGTCCGTGGTCCTGTGGTGACTTAATCCAGTCAAAGTCAGACAATACCC
GGGCCAGGGGCCAGTCAGACTCCAGGCCTTGCTATGACTGGATGAGGAGGGG
CGCACTTTGGGTTTTTCTTGGGCTCTGGTC 3′

Fig. 3. DNA sequences of a fragment exon 6–intron 6 from wild-type and mutant alleles of *Axin*. Underline indicates primers; **bold UPPERCASE** indicates exon 6; UPPERCASE indicates intron 6; ***bold italics*** indicates the IAP insertion site/short direct repeats; lowercase indicates the IAP LTR. (*A*) Wild-type allele. 5′ primer, P23; 3′ primer, G245.R1. (*B*) *Axin*^{Fu} allele, exon 6–5′ LTR. 5′ primer, P23; 3′ primer, RP2. (*C*) *Axin*^{Fu} allele, 3′ LTR–intron 6. 5′ primer, IAP.F; 3′ primer, G245.R1.

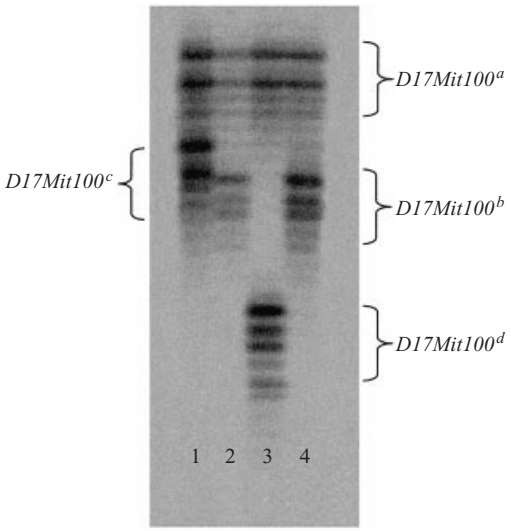

Fig. 4. Five per cent polyacrylamide gel displaying the different alleles of the *D17Mit100* microsatellite locus. Lane 1, *D17Mit100*^{c} [*Axin*^{Fu}]+/*D17Mit100*^{a}+tf; lane 2, *D17Mit100*^{b} *Axin*^{Fu}+/*D17Mit100*^{a}+tf; lane 3, *D17Mit100*^{a} [*Axin*^{Fu}]+/*D17Mit100*^{a}+tf; lane 4, *D17Mit100*^{b} *Axin*^{Fu}+/*D17Mit100*^{a}+tf.

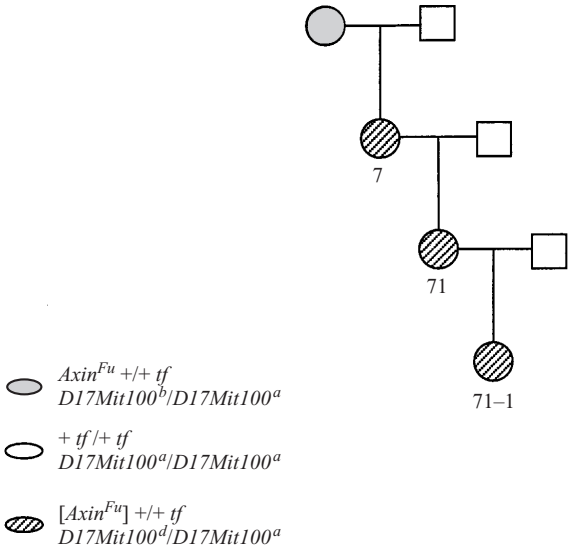

Fig. 5. Pedigree illustrating stable inheritance of [*Axin*^{Fu}] and *D17Mit100*^{d} in experimental line 7.

(Fig. 3). To investigate the region where the IAP was originally inserted we also cloned and sequenced the P23–G245.R1 PCR product from mice carrying the [*Axin*^{Fu}] allele, assuming an equal probability of cloning [*Axin*^{Fu}] and wild-type DNA. Sequences of 20 independent clones from [*Axin*^{Fu}]/+ mice did not demonstrate any difference compared with wild-type *Axin* DNA. The sequence data substantiated our PCR and Southern blot results, in that the IAP is absent in the [*Axin*^{Fu}] chromosome. Furthermore this indicates that mice not only had lost the IAP insert, they appeared to have reverted to the wild-type allele.

https://doi.org/10.1017/S0016672300004651 Published online by Cambridge University Press

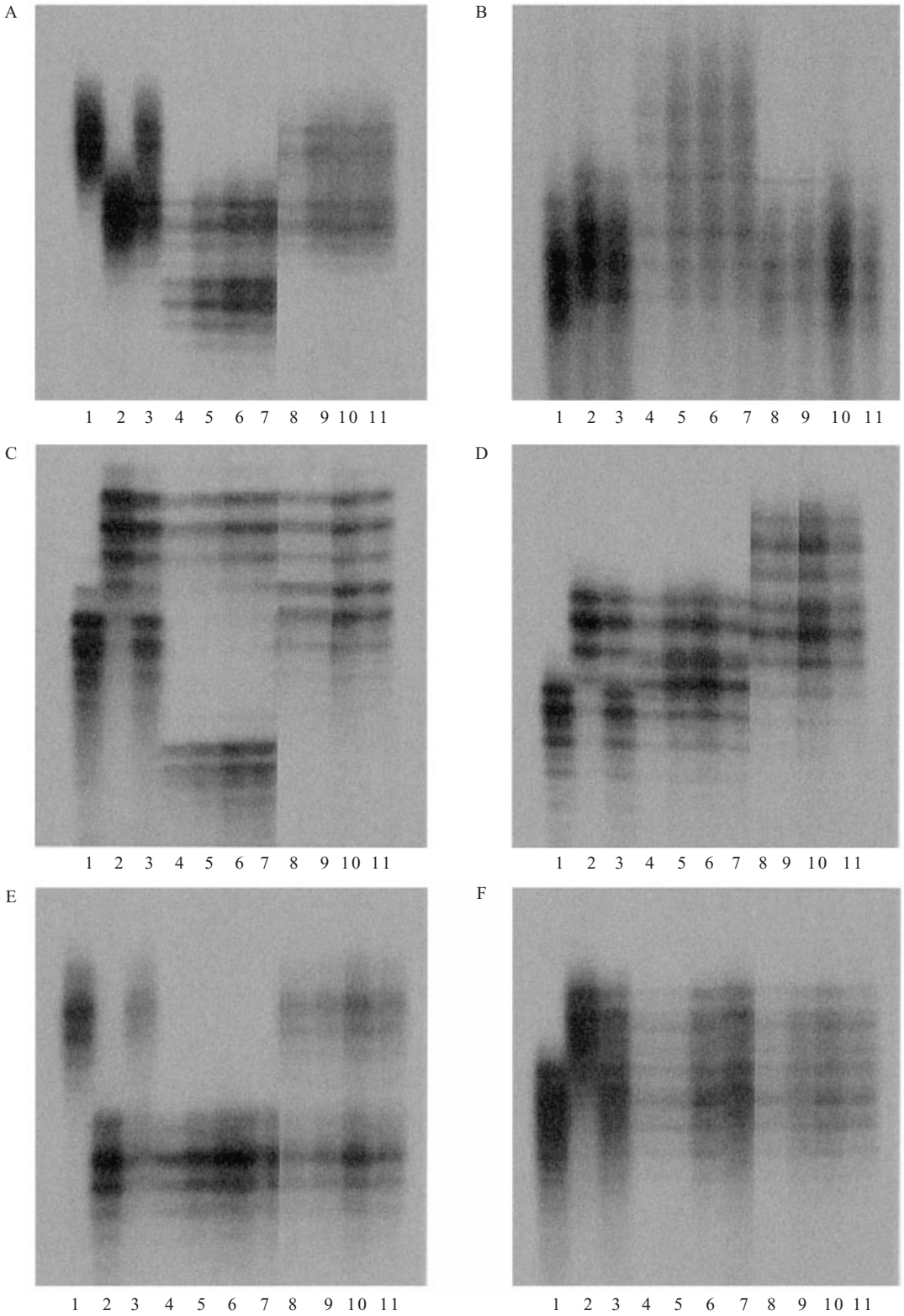

Fig. 6. Five per cent polyacrylamide gel displaying the different alleles in six microsatellite loci. (*A*) *D17Mit19*; (*B*) *D17Mit113*; (*c*) *D17Mit100*; (*D*) *D17Mit173*; (*E*) *D17Mit80*; (*f*) *D17Mit30*. Lane 1, $Axin^{Fu}/Axin^{Fu}$; lane 2, +/+; lane 3, $Axin^{Fu}/+$(f5); lane 4, $[Axin^{Fu}]/+$(f54); lane 5, $[Axin^{Fu}]/+$(f541); lane 6, $[Axin^{Fu}]/+$(f71); lane 7, $[Axin^{Fu}]/+$(f711); lane 8, $[Axin^{Fu}]/+$(m31); lane 9, $[Axin^{Fu}]/+$(f311); lane 10, $[Axin^{Fu}]/+$(f11); lane 11, $[Axin^{Fu}]/+$(m114).

https://doi.org/10.1017/S0016672300004651 Published online by Cambridge University Press

(ii) *Widespread rearrangements in the proximal region of chromosome* 17

In order to trace possible recombination events we investigated microsatellite locus *D17Mit100*, which is particularly close to *Axin*. Analysis of a lambda clone (λwt9) demonstrated that the microsatellite is located less than 5 kb upstream from the *Axin* promoter (data not shown). Investigation of the *D17Mit100* locus from chromosomes carrying [$Axin^{Fu}$] revealed that, in addition to the spontaneous disappearance of the IAP, two novel alleles (Fig. 4) had emerged which were distinct from both parental alleles *D17Mit100*^{a} (chromosome with *tf*) and *D17Mit100*^{b} (chromosome with $Axin^{Fu}$). These two novel alleles are specific for chromosomes carrying [$Axin^{Fu}$]. In the 22 studied cases where the IAP disappeared from the *Axin* locus, 14 instances of the *D17Mit100*^{c} allele and 8 cases of the *D17Mit100*^{d} allele were observed.

The concomitant and independent change in the tightly linked $Axin^{Fu}$ and *D17Mit100*^{b} alleles is illustrated for instance in experimental line 5. Six offspring resulting from a cross between female 5 ($Axin^{Fu}+/+tf$) and male m02 ($+tf/+tf$) have been studied in detail. Four phenotypically normal offspring (f51, f52, f53, f54) lost the mutation-specific IAP and the parental microsatellite allele *D17Mit100*^{b} was replaced by the novel allele *D17Mit100*^{d}. These mice demonstrated stable inheritance of *D17Mit100*^{d} and [$Axin^{Fu}$] into the next generation. Two other offspring (f56 and f57) were phenotypically mutant and maintained the IAP (hence mutant $Axin^{Fu}$ allele). These mice carried the parental *D17Mit100*^{b} allele and displayed stable inheritance of both the microsatellite and $Axin^{Fu}$ alleles. Another example of stable transmission of $Axin^{Fu}$ and *D17Mit100*^{d} is shown in the pedigree of experimental line 7 (Fig. 5).

To characterize the variation at the *D17Mit100* locus, we cloned and sequenced the *D17Mit100* alleles (GenBank accession numbers AF135045, AF135046, AF135047 and AF135048). All alleles of *D17Mit100* were comprised of two sets of dinucleotide repeats: d(CT)$_n$ in the 5′ portion and d(CA)$_n$ in the 3′ portion. While the 5′ CT dinucleotide composition was constant in *D17Mit100* alleles *a* (136 bp), *c* (130 bp) and *d* (120 bp) being equal to d(CT)$_{11}$, allele *D17Mit100*^{b} (128 bp) displayed an extra two dinucleotide repeats, d(CT)$_{13}$. In the parental alleles *D17Mit100*^{a} and *D17Mit100*^{b}, the number of CA repeats in the 3′ portion was d(CA)$_{21}$ and d(CA)$_{15}$ respectively. In the chromosome with [$Axin^{Fu}$], allele *D17Mit100*^{b} was always replaced with either of the novel alleles. The novel alleles were characterized by the disappearance of the extra two CT dinucleotides present in allele *b* and variation in the number of 3′ CA dinucleotide repeats. In *D17Mit100*^{c} the number of the CA repeats increased, d(CA)$_{18}$, as with *D17Mit100*^{b} causing expansion of the allele. On the other hand, in the *D17Mit100*^{d} allele the CA dinucleotide repeats were reduced, d(CA)$_{13}$, resulting in contraction of the allele.

To determine whether any other loci were involved, we investigated 10 additional microsatellite markers both proximal and distal to *Axin*. These markers span the proximal region of chromosome 17 from *D17Mit19* (3·0 cM) to *D17Mit191* (17·2 cM). Surprisingly, in the majority of microsatellite loci, we found novel alleles which were not observed in either parent (Fig. 6).

Parental and novel microsatellites are shown in six loci – *D17Mit19*, *D17Mit113*, *D17Mit100*, *D17Mit173*, *D17Mit80* and *D17Mit30* – which were ordered identically on each gel (Fig. 6 *A–F*). Lanes 1 and 2 on the gels represent homozygotes ($Axin^{Fu}+/Axin^{Fu}+$) and male 02 ($+tf/+tf$). Lane 3 shows heterozygous female 5 ($Axin^{Fu}+/+tf$). Thus, lane 1 shows the microsatellite pattern of haplotype *b* on the chromosome carrying $Axin^{Fu}$ and lane 2 indicates haplotype *a* on the chromosome carrying *tf*. All other lanes represent different heterozygotes and hence represent two haplotypes. No novel alleles were observed in the *D17Mit30* locus, which is likely to be beyond the area of microsatellite variation.

Lanes 4–7 show mice which have lost the IAP ([$Axin^{Fu}$]$+/+tf$) and have haplotype *d* on the chromosome carrying [$Axin^{Fu}$]. The *d* designation was used to indicate the presence of allele *D17Mit100*^{d} in all mice carrying this haplotype. Lanes 8–11 represent animals who also lost IAP ([$Axin^{Fu}$]$+/+tf$) but have haplotype *c* on the chromosome carrying [$Axin^{Fu}$]. In this case the *c* designation was used to indicate the presence of the *D17Mit100*^{c} allele in all mice carrying haplotype *c*.

Lanes 3 and 4 represent parent (f5, [$Axin^{Fu}$]/+) and offspring (f54, [$Axin^{Fu}$]/+) respectively. Interestingly in all cases the microsatellites in the novel haplotype regions of the [$Axin^{Fu}$]/+ mice were not previously observed in parental stocks. Loss of the IAP from the mutant allele and concomitant changes in numerous microsatellites from the same chromosome in [$Axin^{Fu}$]/+ mice strongly suggest a connection between these two events. Lanes 4 and 5, 6 and 7, 8 and 9, and 10 and 11 also show parent and offspring pairs, all being [$Axin^{Fu}$]/+ (Fig. 6). The former two pairs carry haplotype *d* and the latter two, haplotype *c*. Thus, identical sets of microsatellites have been observed in haplotype *c* or *d*, of independent origin. These data demonstrate the stability of inheritance of the novel microsatellites.

Essentially two new haplotypes carrying distinct sets of novel microsatellite alleles appeared during this investigation that covered significant lengths across the proximal region of chromosome 17. The parental chromosomes (Fig. 7 *A*, *B*) carrying *tf* (haplotype *a*)

https://doi.org/10.1017/S0016672300004651 Published online by Cambridge University Press

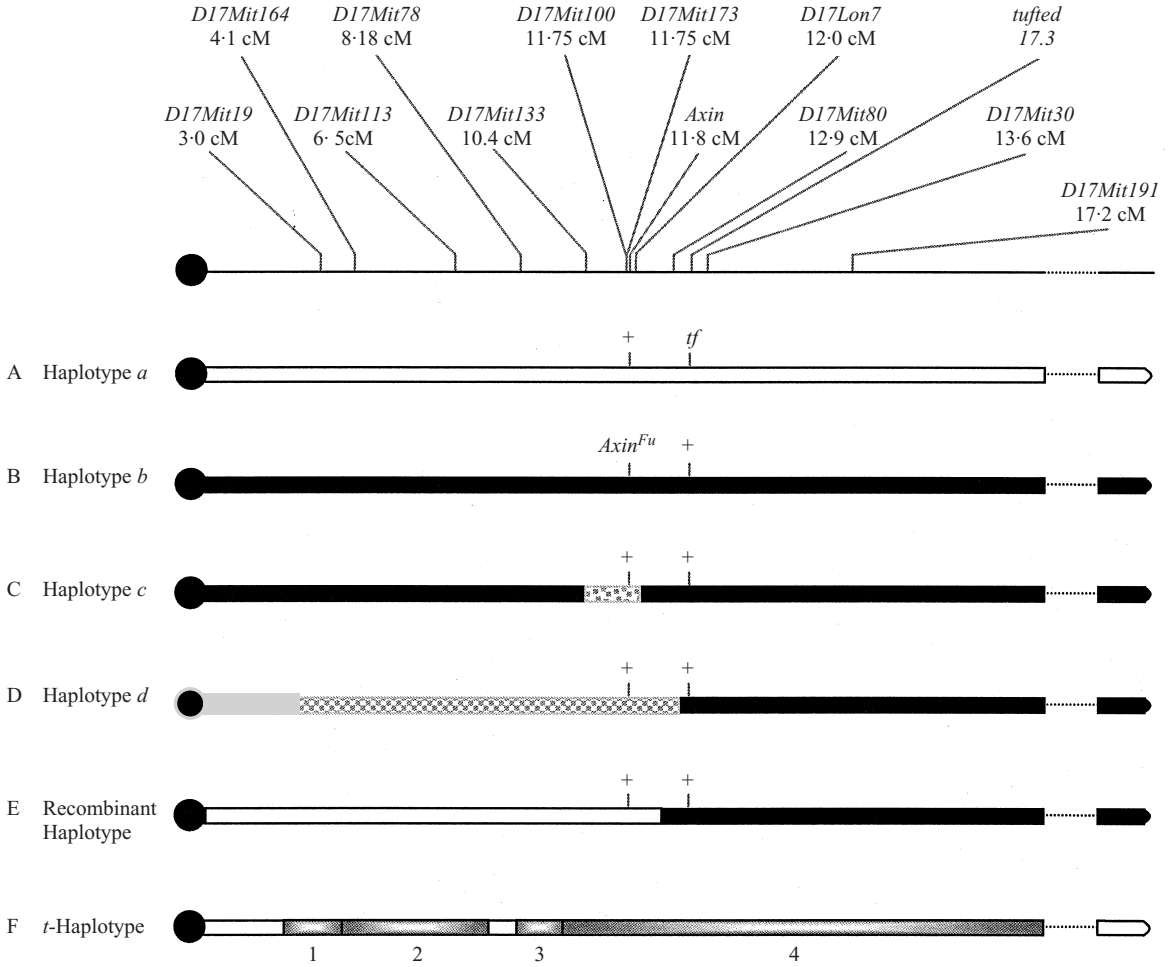

Fig. 7. Genetic map of the proximal region of chromosome 17 indicating the relative positions of the studied microsatellite loci with the *Axin* and *tufted* loci. (*A*) Haplotype *a*, representative of chromosomes carrying the wild-type *Axin* and *tufted* alleles. (*B*) Haplotype *b*, representative of chromosomes carrying the mutant $Axin^{Fu}$ allele and wild-type allele at the *tufted* locus. (*C*) Haplotype *c*, representative of chromosomes carrying the [$Axin^{Fu}$] allele designated as + and the novel $D17Mit100^{c}$ allele. This haplotype is distinguishable from either parental haplotype *a* or *b* by a unique region (stippled box) defined by the appearance of novel alleles across several microsatellite loci. (*D*) Haplotype *d*, representative of inactive chromosomes carrying the novel $D17Mit100^{d}$ allele. This haplotype is also distinguishable from either parental haplotype *a* or *b* by a unique region (hatched box) defined by the appearance of numerous novel alleles across numerous microsatellite loci. Grey box indicates region not studied. (*E*) Recombinant haplotype, representative of a chromosome where reciprocal exchange has occurred between the *Axin* and *tufted* loci. The structure of chromosome 17 in recombinants is clearly distinguishable from the corresponding chromosome in mice carrying [$Axin^{Fu}$] allele. (*F*) *t*-Haplotype. Numbers indicate the four inversions.

Table 1. *Microsatellite composition of haplotypes a, b and two independent novel c haplotypes*

Mouse	PCR phenotype	Chromosome	Haplotype	Microsatellite alleles	
m02	F	$+tf$	*a*	$D17Mit100^{a}$	$D17Mit173^{a}$
f5	FS	$Axin^{Fu}+$	*b*	$D17Mit100^{b}$	$D17Mit173^{b}$
m31	F	[$Axin^{Fu}$]+	*c*	$\underline{D17Mit100^{c}}$	$\underline{D17Mit173^{c}}$
f11	F	[$Axin^{Fu}$]+	*c*	$\underline{D17Mit100^{c}}$	$\underline{D17Mit173^{c}}$

Underlining indicates expansion of the microsatellite allele.

and $Axin^{Fu}$ (haplotype *b*) were distinct from chromosomes carrying [$Axin^{Fu}$] with either haplotype *c* or haplotype *d* (Fig. 7*C*, *D*). The altered region of the novel haplotype *c* is located between markers *D17Mit133* (10·4 cM) and *D17Mit80* (12·9 cM), covering the *Axin* locus. Within this region, two studied

https://doi.org/10.1017/S0016672300004651 Published online by Cambridge University Press

Table 2. *Microsatellite composition of haplotypes a, b and two independent novel d haplotypes*

Mouse	PCR phenotype	Chromosome	Haplotype	Microsatellite alleles
m02	F	$+tf$	*a*	$D17Mit19^a$ $D17Mit113^a$ $D17Mit100^a$ $D17Mit173^a$ $D17Mit80^a$
f5	FS	$Axin^{Fu}+$	*b*	$D17Mit19^b$ $D17Mit113^b$ $D17Mit100^b$ $D17Mit173^b$ $D17Mit80^b$
f54	F	$[Axin^{Fu}]+$	*d*	$\mathbf{D17Mit19^d}$ $\underline{D17Mit113^a}$ $\mathbf{D17Mit100^d}$ $\underline{D17Mit173^d}$ $\mathbf{D17Mit80^a}$
f71	F	$[Axin^{Fu}]+$	*d*	$\mathbf{D17Mit19^d}$ $\underline{D17Mit113^a}$ $\mathbf{D17Mit100^d}$ $\underline{D17Mit173^d}$ $\mathbf{D17Mit80^a}$

Underlining indicates expansion of the microsatellite allele.
Bold indicates contraction of the microsatellite allele.

microsatellite markers (*D17Mit100* and *D17Mit173*) show alleles that are different from alleles *a* and *b*, due to expansion of their sequences (Table 1). In all cases, a novel allele specific for a particular microsatellite locus was identical to the novel allele at the same locus in haplotypes of independent origin (Table 1). The length of the aberrant region covered by the haplotype *c* is estimated to be 2·5 cM.

The length of the altered component of the novel haplotype *d* was much larger, covering the region between *D17Mit19* (3·0 cM) and *tf* (13·3 cM). However, the position of the proximal end of haplotype *d* has not been resolved, due to a lack of available polymorphic microsatellites between the centromere and *D17Mit19*. From eight novel microsatellites within haplotype *d*, there were five cases of microsatellite expansion and three cases of contraction (Table 2, not all studied microsatellites are shown). In the *D17Mit80* locus, however, it seems that the $Axin^{Fu}$ specific allele has been replaced by the wild-type allele. Nevertheless, as for haplotype *c*, in haplotype *d* there was an altered region where all studied microsatellite markers were different from alleles *a* and *b*. Furthermore in all cases for haplotype *d*, as for haplotype *c*, a novel allele specific for a particular microsatellite locus was identical to the novel allele at the same locus in haplotypes of independent origin (Table 2).

The analysis shows that chromosomes with novel haplotypes *c* and *d* were identical to parental haplotype *b*, beyond the regions changed in the novel haplotypes. This proves that $[Axin^{Fu}]/+$ mice with either haplotype *c* or *d* inherited the parental chromosomes that carried the mutant $Axin^{Fu}$ allele in the previous generation (haplotype *b*). The novel haplotypes *c* and *d* were always stable during transmission to the next generation (Fig. 6).

During this investigation we isolated 13 recombinants among 1380 studied offspring, of which at least eight occurred within the *Axin–tufted* interval while the remaining five have not been tested for the presence of *tufted* or other markers. Recombinants were easily distinguished from mice which had lost the mutation-specific IAP, by the presence of chromosomes which combine both parental haplotypes *a* and *b* (Fig. 7*E*). In addition, recombinants do not display the novel alleles that are typical for haplotypes *c* and *d*. Thus, as expected, all investigated recombinants show reciprocal exchange between the parental chromosomes.

4. Discussion

This investigation provides two major observations. Primarily we show that spontaneously normal mice arise from mutant parents through disappearance of the IAP from intron 6 of mutant $Axin^{Fu}$ allele. It is indicated by four independent lines of evidence: genetic data, PCR, Southern blot and direct sequencing of the region covering the IAP insertion. This leaves no doubt that there was loss of IAP from the locus in cases when the fused phenotype disappeared in offspring which themselves could no longer pass on the mutant allele to the next generation (Belyaev *et al*., 1981). Furthermore we show the simultaneous emergence of several novel microsatellite alleles in the area surrounding the *Axin* locus in mice which lost the IAP. It is not feasible to assume that these two major events are unrelated. Hence we believe that disappearance of the IAP from intron 6 of the $Axin^{Fu}$ allele and the formation of novel microsatellite alleles in several studied loci on chromosome 17 are the product of a single event.

The question may arise as to whether the novel haplotypes could have been present in parental strains and we can indicate several reasons why in principle this could not be. First, non-fused, non-tufted mice ($[Axin^{Fu}]+/+tf$) were found in the $Axin^{Fu}+/+tf \times +tf/+tf$ cross. In this cross, one parent was always phenotypically fused and the other parent displayed the tufted phenotype. In this respect, as phenotypically fused parents were strictly selected for this cross, any mice that may have had $[Axin^{Fu}]$ and a novel haplotype, being phenotypically normal, would never have been used in the breeding programme. With regard to the $+tf/+tf$ parents, the microsatellite study provides conclusive proof that the chromosome which carried the *tf* allele in $[Axin^{Fu}]+/+tf$ mice,

https://doi.org/10.1017/S0016672300004651 Published online by Cambridge University Press

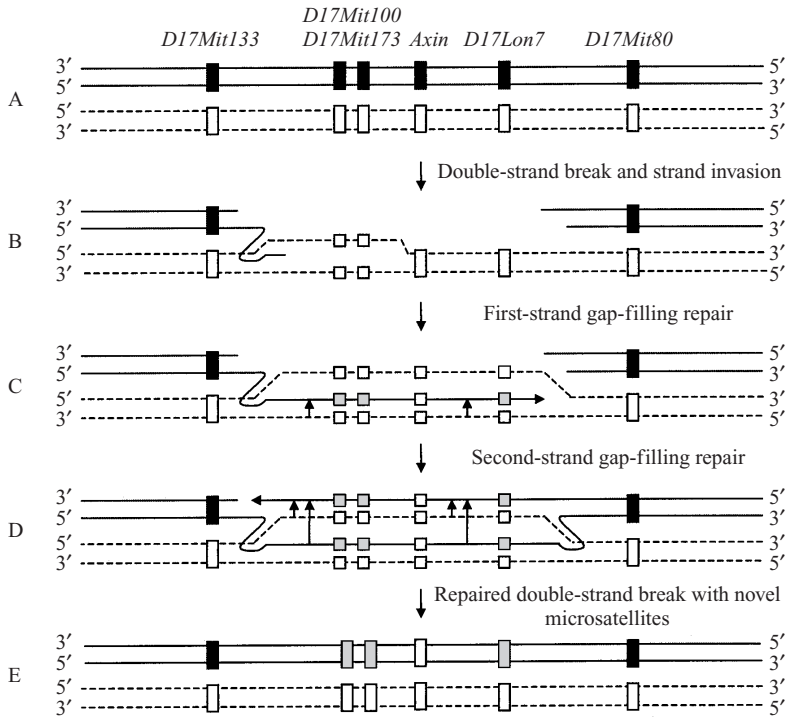

Fig. 8. Double-strand break repair model with synthesis-dependent strand annealing accounting for widespread rearrangement. (*A*) Parental DNA. Black boxes on continuous lanes represent microsatellite alleles typical for chromosomes carrying $Axin^{Fu}$ at the indicated loci. Unshaded boxes and dashed lines represent microsatellite alleles typical for chromosome carrying *tufted* at the indicated loci. While *D17Mit100* and *D17Mit173* are both located at 11·75 cM, their relative position on the map is unknown. (*B*) Double-strand break allows a free end to invade the homologous duplex and pair with a complementary strand. This does not result in genetic exchange with the formation of a Holliday junction and predicts that the template strands remain unaltered. (*C*) First-strand gap-filling repair progresses across the region of the double-strand break using the complementary strand as a template (short arrows) and uniting with the opposite end of the break. Errors occur at microsatellite loci across this region (grey squares) compromising fidelity of synthesis of the nascent microsatellite. (*D*) Second-strand gap-filling repair may occur using either nascent repaired strand (long arrows) or the complementary strand from the homologous chromosome (short arrows) as a template. Synthesis of the second strand may proceed using the complementary strand of the homologous chromosome as a template. This would require the independent production of identical mutations in each microsatellite locus for both strands (grey squares). Otherwise, the production of different alleles in the studied loci would lead to the appearance of more than the two observed haplotypes. More likely, the newly synthesized first strand may be used as a template to produce an exact copy of the microsatellite mutation in the second strand. (*E*) The repaired double-strand break contains novel alleles in the microsatellite loci (grey rectangles) and a wild-type *Axin* gene (top). The chromosome carrying *tufted* remains unaltered (bottom). While this figure has been used to illustrate the conversion mechanism resulting in the formation of haplotype *c*, it is equally viable to describe formation of haplotype *d*.

displayed only the typical *a* haplotype, indicating inheritance of a normal *tf* chromosome. Without exception, no novel haplotypes were observed on the *tf* chromosome. Collectively these observations oppose any suggestion that the novel haplotypes were present in parental strains and argue in favour of spontaneous loss of the mutation specific IAP with concomitant appearance of the novel haplotypes.

Another general argument is that all mice with the [$Axin^{Fu}$] allele carried either novel haplotype *c* or *d*, while none of the studied $Axin^{Fu}+/+tf$ or $+tf/+tf$ mice ever had these haplotypes.

Finally, the structure of both *c* and *d* haplotypes clearly indicates that they originated from an $Axin^{Fu}$ chromosome as the microsatellite composition of these chromosomes beyond the altered region surrounding *Axin* was identical to parental $Axin^{Fu}$ chromosomes. This is evidence that both novel haplotypes originated in progeny of $Axin^{Fu}+/+tf$ mice but not in the tufted strain (TF/Le).

As the novel haplotypes were never observed in parental stocks the appearance of novel haplotypes in all mice who lost the IAP cannot be explained through a mix-up of animals or samples. All progeny investigated in this study came from the cross $Axin^{Fu}+/+tf\times+tf/+tf$, as described in Section 2. During this work only these two strains were available.

The size of the region involved in reorganization varies from 2·5 cM in the case of the haplotype *c* to at least 9·9 cM for the haplotype *d*, where the proximal end has not yet been finally localized. Although the molecular mechanism which could explain these observations remains to be verified, we suggest a possible model which corresponds with our data.

https://doi.org/10.1017/S0016672300004651 Published online by Cambridge University Press

As haplotype *c* is identical to haplotype *b* except for the altered region (Fig. 7*C*), double recombination cannot explain the appearance of this haplotype because the altered region is different from both parental haplotypes *a* or *b*. Classical double recombination could not account for the spontaneous and concomitant emergence of the novel alleles in the three linked microsatellite loci (*D17Mit100*, *D17Mit173* and *D17Lon7*), while *Axin^{Fu}* was substituted by the wild-type allele. Hence, the experimental data distinguish between double recombination and the formation of the novel haplotypes. Haplotype *d* shows similar features to haplotype *c*. Nevertheless there are distinctive differences including greater length and location of the ends of the altered region. The novel alleles were not observed in all studied loci. At least in locus *D17Mit80*, the allele typical for the chromosome carrying *Axin^{Fu}* has been replaced by the allele typical for the chromosome carrying *tufted*.

With the exclusion of double recombination as a means of explaining the widespread reorganization, a conceivable way to interpret these results suggests the involvement of a gene conversion-like process that has the capacity to cover vast regions of chromosome.

The number of investigated mammalian systems showing conversion-like events is growing steadily (Pittman & Schimenti, 1998). Several models have been suggested for double-strain break repair (Szostak *et al*., 1983; Engels *et al*., 1990; Giver & Grosovsky, 1997). One model, the synthesis-dependent strand annealing model describing gene conversion (Fig. 8), may account at least in part for the reorganization of chromosome 17 (Nassif *et al*., 1994; Richard *et al*., 1999). As follows from the model, a double-strand break induces strand invasion followed by DNA synthesis, which uses intact wild-type DNA strands as a template for repair. In the synthesis-dependent strand annealing model strand recombination does not occur and there is no classical Holliday structure (Richard *et al*., 1999). Therefore the model predicts that the wild-type chromosome remains unchanged (Nassif *et al*., 1994; Richard *et al*., 1999). The newly repaired chromosome will lose *Axin^{Fu}*, which is replaced by the wild-type allele, while areas beyond the double-strand break should not be altered. However, within the repaired region, mutations may occur during the resynthesis of DNA, particularly in microsatellite loci. It has been reported that the presence of trinucleotide repeats sharply increases the frequency of mutation in the repaired area (Richard *et al*., 1999). It has been proposed that gene conversion might introduce mutations within the conversion tract due to error-prone gap-filling synthesis (Ninio, 1996; Giver & Grosovsky, 1997). The stability of replication of dinucleotide repeats in *Drosophila* has been shown to be under special pressure during gene conversion in certain genotypes (Flores & Engels, 1999). This argues that new alleles in the studied microsatellite loci may have arisen due to error-prone gap repair during gene conversion. Our observations are consistent with such a model.

The model also indicates that both newly repaired DNA strands contain identical mutant alleles in several microsatellite loci (Fig. 8). This hypothetical assumption is based on the fact that the studied mice, which lost IAP, had only two haplotypes, *c* or *d*. Many more haplotypes would be expected if mutations were not identical but arose randomly in non-related microsatellite loci. The reason why only two repeatable haplotypes were observed remains to be addressed.

Thus, the observed phenomena can be explained by imperfect and repeatable gene conversion-like events, assigned to specific locations in chromosome 17. However, it is not clear why mutations in repaired complementary DNA strands should arise in a coordinated manner.

One difficulty in accepting the suggested mechanism is that the conversion tracts observed in haplotypes *c* and *d* are extremely long, indicating that these events have spread across millions of base pairs. Conversion events described so far usually do not spread beyond a 1 cM interval (Giver & Grosovsky, 1997). Results obtained from yeast demonstrate that conversion tracts frequently extended across significant lengths from both sides of a recombination-stimulating sequence, which is considered to be the cause of a double-strand break (Voelkel-Meiman & Roeder, 1990). It is unknown whether one integrated event or a series of simultaneous gene conversions within the same region would generate each novel haplotype. Nonetheless the likelihood of a single integrated event is much higher. If so, then a continuous error-prone conversion tract could better explain the unusual inheritance of the *Axin^{Fu}* allele and the studied microsatellites. Data confirming multiple simultaneous changes in genomes have steadily accumulated during the last decade (Caporale, 1999).

As mentioned in this paper a significant number of independent IAP losses have been observed. In all cases, loss of the IAP precisely reverted the DNA sequence of the *Axin^{Fu}* allele to wild-type. Similar observations have been made with the long terminal repeat (LTR)-containing retrotransposon gypsy, which demonstrates precise excision from the *forked* and *cut* loci in a genetically unstable *Drosophila melanogaster* strain (Kuzin *et al*., 1994). However, gene conversion was ruled out in this case as precise excision events were occurring in homozygotes. Excision of LTR-containing elements is often accomplished through homologous recombination between LTRs. These events are identified by the presence of a solitary LTR that remains following the recombination event (Copeland *et al*., 1983). Disappearance of the IAP from the *Axin^{Fu}* allele cannot

https://doi.org/10.1017/S0016672300004651 Published online by Cambridge University Press

be explained through homologous recombination as a solitary LTR is not observed in [$Axin^{Fu}$] because the sequence reverts precisely to wild-type.

Acceptance of the double-strand break model as a mechanism for the reversion process raises a question concerning the frequency of double-strand breaks in the proximal region of chromosome 17. Numerous deletions, duplications, unequal recombinations and translocations have been found in this region (Silver, 1985; Sarvetnick *et al.*, 1986; Bucan *et al.*, 1987; Lyon, 1992). Remarkably, this portion of chromosome 17 is also covered by *t*-haplotypes, which consist of four inversions (Fig. 6*F*). Non-homologous recombination between different *t*-haplotypes and wild-type chromosomes regularly produces aberrant *t*-haplotypes. Interestingly, the proximal portion of the altered region in haplotype *c* maps relatively close to the proximal end of the fourth inversion of the *t*-haplotypes. Moreover the proximal region of haplotype *d* is located near the proximal end of the first *t*-haplotype inversion. Hypothetically one could suggest that the borders of *t*-haplotypes might coincide with double-strand break hotspots. Specific DNA sequence composition may promote these hotspots (Wahls, 1998). While gene conversion is known for its involvement in double-strand break repair, it is also a common form of genetic exchange across at least one of the four *t*-associated inversions (Hammer *et al.*, 1991).

The initial objective of this study was to understand the unusual inheritance of the $Axin^{Fu}$ mutation in mice. We now realize that this mutation serves as a useful marker to reveal widespread rearrangements that cover a significant region of chromosome 17.

We thank R. Holliday, A. McLaren and S. Tilghman for valuable discussions. We are also grateful to a reviewer for constructive advice and exceptional insight. This work was supported by Australian Research Council (A.R.). W.D.F. was supported by an Australian Postgraduate Award.

References

Belyaev, D. K., Ruvinsky, A. O. & Borodin, P. M. (1981). Inheritance of alternative states of the fused gene in mice. *Journal of Heredity* **72**, 107–112.

Bollag, R. J., Elwood, D. R., Tobin, E. D., Godwin, A. R. & Liskay, R. M. (1992). Formation of heteroduplex DNA during mammalian intrachromosomal gene conversion. *Molecular and Cellular Biology* **12**, 1546–1552.

Bucan, M., Herrmann, B. G., Frischauf, A. M., Bautch, V. L., Bode, V., Silver, L. M., Martin, G. R. & Lehrach, H. (1987). Deletion and duplication of DNA sequences is associated with the embryonic lethal phenotype of the t9 complementation group of the mouse t complex. *Genes and Development* **1**, 376–385.

Caporale, L. H. (1999). Chance favors the prepared genome. In *Molecular Strategies in Biological Evolution* (ed. L. H. Caporale). *Annals of the New York Academy of Sciences* **870**, 1–22.

Copeland, N. G., Hutchison, K. W. & Jenkins, N. A. (1983). Excision of the DBA ecotropic provirus in dilute coat-colour revertants of mice occurs by homologous recombination involving the viral LTRs. *Cell* **33**, 379–387.

Dunn, L. C. & Gluecksohn-Waelsch, S. (1954). A genetical study of the mutation 'Fused' in the house mouse, with evidence concerning its allelism with a similar mutation 'Kink'. *Journal of Genetics* **52**, 383–391.

Engels, W. R., Johnson-Schlitz, D. M., Eggleston, W. B. & Sved, J. (1990). High-frequency P element loss in Drosophila in homolog dependent. *Cell* **62**, 515–525.

Flores, C. & Engels, W. (1999). Microsatellite instability in *Drosophila* spellchecker1 (MutS homolog) mutants. *Proceedings of the National Academy of Sciences of USA* **96**, 2964–2969.

Giver, C. R. & Grosovsky, A. J. (1997). Single and coincident intragenic mutations attributable to gene conversion in a human cell lane. *Genetics* **146**, 1429–1439.

Greenspan, R. J. & O'Brien, M. C. (1986). Genetic analysis of mutations at the fused locus in the mouse. *Proceedings of the National Academy of Sciences of the USA* **83**, 4413–4417.

Hammer, M. F., Bliss, S. & Silver, L. M. (1991). Genetic exchange across a paracentric inversion of the mouse *t* complex. *Genetics* **128**, 799–812.

Hart, M. J., de los Santos, R., Albert, I. N., Rubinfeld, B. & Polakis, P. (1998). Downregulation of beta-catenin by human Axin and its association with the APC tumor suppressor, beta-catenin and GSK3 beta. *Current Biology* **8**, 573–581.

Holliday, R. (1964). A mechanism for gene conversion in fungi. *Genetical Research* **5**, 282–304.

Hsu, W., Zeng, L. & Costantini, F. (1999). Identification of a domain of Axin that binds to the serine/threonine protein phosphatase 2A and a self-binding domain. *Journal of Biological Chemistry* **274**, 3439–3445.

Ikeda, S., Kishida, S., Yamamoto, H., Murai, H., Koyama, S. & Kikuchi, A. (1998). Axin, a negative regulator of the Wnt signaling pathway, forms a complex with GSK-3beta and beta-catenin and promotes GSK-3beta-dependent phosphorylation of beta-catenin. *EMBO Journal* **17**, 1371–1384.

Kishida, S., Yamamoto, H., Ikeda, S., Kishida, M., Sakamoto, I., Koyama, S. & Kikuchi, A. (1998). Axin, a negative regulator of the Wnt signaling pathway, directly interacts with adenomatous polyposis coli and regulates the stabilization of beta-catenin. *Journal of Biological Chemistry* **273**, 10823–10826.

Kuzin, A. B., Lyubomirskaya, N. V., Khudaibergenova, B. M., Ilyin, Y. V. & Kim, A. I. (1994). Precise excision of the retrotransposon gypsy from the forked and cut loci in genetically unstable *D. melanogaster* strain. *Nucleic Acids Research* **22**, 4641–4645.

Lyon, M. F. (1992). Deletion of mouse t-complex distorter-1 produces an effect like that of the t-form of the distorter. *Genetical Research* **59**, 27–33.

Marchuk, D., Drumm, M., Saulino, A. & Collins, F. S. (1991). Construction of T-vectors, a rapid and general system for direct cloning of unmodified PCR products. *Nucleic Acids Research* **19**, 1154.

Nassif, N., Penney, J., Pal, S., Engels, W. R. & Gloor, G. B. (1994). Efficient copying of nonhomologous sequences from ectopic sites via P-element-induced gap repair. *Molecular and Cellular Biology* **14**, 1613–1625.

Ninio, J. (1996). Gene conversion as a focusing mechanism for correlated mutations: a hypothesis. *Molecular and General Genetics* **251**, 503–508.

Perry, W. L. 3rd, Vasicek, T. J., Lee, J. J., Rossi, J. M., Zeng, L., Zhang, T., Tilghman, S. M. & Costantini, F. (1995). Phenotypic and molecular analysis of a transgenic insertional allele of the mouse Fused locus. *Genetics* **141**, 321–332.

Pittman, D. L. & Schimenti, J. C. (1998). Recombination in the mammalian germ lane. *Current Topics in Developmental Biology* **37**, 1–35.

Reed, S. C. (1937). The inheritance and expression of Fused, a new mutation in the house mouse. *Genetics* **22**, 1–13.

Richard, G. F., Dujon, B. & Haber, J. E. (1999). Double-strand break repair can lead to high frequencies of deletions within short CAG/CTG trinucleotide repeats. *Molecular and General Genetics* **261**, 871–882.

Ruvinsky, A. (1987). Inheritance of dominant genes with variable penetrance: an evolutionary aspect. *Journal of Animal Breeding and Genetics* **105**, 103–111.

Ruvinsky, A., Agulnik, A., Agulnik, S. & Rogachova, M. (1991). Functional analysis of mutations of murine Chromosome 17 with the use of tertiary trisomy. *Genetics* **127**, 781–788.

Sarvetnick, N., Fox, H. S., Mann, E., Mains, P. E., Elliott, R. W. & Silver, L. M. (1986). Nonhomologous pairing in mice heterozygous for a *t* haplotype can produce recombinant chromosomes with duplications and deletions. *Genetics* **113**, 723–734.

Silver, L. M. (1985). Mouse *t* haplotypes. *Annual Review of Genetics* **19**, 179–208.

Szostak, J. W., Orr-Weaver, T. L., Rothstein, R. J. & Stahl, F. W. (1983). The double-strand-break repair model for recombination. *Cell* **33**, 25–35.

Vasicek, T. J., Zeng, L., Guan, X. J., Zhang, T., Costantini, F. & Tilghman, S. M. (1997). Two dominant mutations in the mouse fused gene are the result of transposon insertions. *Genetics* **147**, 777–786.

Voelkel-Meiman, K. & Roeder, G. S. (1990). Gene conversion tracts stimulated by HOT1-promoted transcription are long and continuous. *Genetics* **126**, 851–867.

Wahls, W. P. (1998). Meiotic recombination hotspots: shaping the genome and insights into hypervariable minisatellite DNA change. *Current Topics in Developmental Biology* **37**, 37–75.

Zeng, L., Fagotto, F., Zhang, T., Hsu, W., Vasicek, T. J., Perry, W. L. 3rd, Lee, J. J., Tilghman, S. M., Gumbiner, B. M. & Costantini, F. (1997). The mouse Fused locus encodes Axin, an inhibitor of the Wnt signaling pathway that regulates embryonic axis formation. *Cell* **90**, 181–192.